DEVELOPMENT OF REGIONAL PHASE TOMOGRAPHIC ATTENUATION MODELS FOR EURASIA

Thorne Lay[1], Xiao-Bi Xie[1], Xiaoning (David) Yang[2], Steven R. Taylor[2], and W. Scott Phillips[2]

Los Alamos National Laboratory[1] and University of California, Santa Cruz[2]

Sponsored by National Nuclear Security Administration
Office of Nonproliferation Research and Engineering
Office of Defense Nuclear Nonproliferation

Contract Nos. DE-FC52-05NA26606[1] and W-7405-ENG-36[2]

ABSTRACT

The national laboratories are currently calibrating regional seismic discriminants for Eurasia. The Magnitude and Distance Amplitude Correction (MDAC) (Taylor and Hartse, 1998; Taylor et al., 2002, Walter and Taylor, 2002) is being used to correct amplitudes for discriminants. The MDAC methodology corrects regional seismic amplitudes by assuming physically based propagation and earthquake source models. Regional phase attenuation models at 1 Hz developed by Los Alamos National Laboratory (LANL) are currently being used in eastern Asia to perform MDAC corrections. In other regions, one-dimensional Q models are used. These tomographic models need to be extended to all of Eurasia to improve nuclear explosion monitoring capabilities to wider areas. We are expanding existing 1 Hz regional phase (Pn, Pg, Sn, Lg) tomographic attenuation models for Eurasia. The models will be integrated into the National Nuclear Security Administration (NNSA) Knowledge Base and will be used in the MDAC station calibration for development of regional seismic discriminants. Accurately accounting for regional phase geometrical spreading is critical for development of useful anelastic attenuation models, particularly for upper mantle diving waves (Pn and Sn). The MDAC approach currently uses a simple representation of regional phase geometrical spreading that performs well between local to near-regional (200–400 km) and far-regional to teleseismic transition zone regions (< 16–18^{o}). In order to seamlessly tie regional MDAC to local and teleseismic distances, it is important to devise strategies to account for geometrical effects in these transition zone regions. We will focus our work on the 1 Hz Pn phase and examine whether combined empirical and model-based approaches can be used to improve geometric spreading corrections in different geophysical regions. As is well known, Pn is an extremely important phase in seismic event identification and the goal of this work is to improve its efficacy. One of the questions we hope to answer is whether it is adequate to continue to use the simple formulation currently used supplemented by amplitude tomography and possibly station-centric amplitude kriging or could a set of model-based corrections be formed from geophysical models being compiled for Eurasia as part of the NNSA program. The metric to be used to test these different methodologies would be event classification error rates using the extensive ground truth dataset compiled by the NNSA laboratories.

OBJECTIVES

The project has the following research objectives:

- Develop regional phase (Pn, Pg, Sn, Lg) tomographic attenuation maps for Eurasia at 1 Hz.
- Develop combined empirical/model-based approaches for representation of 1 Hz Pn (and Sn) wave geometrical spreading factors at transition zone regions (local to regional and far regional to teleseismic).

RESEARCH ACCOMPLISHED

Bayesian Attenuation Tomography

We have added the ability to incorporate Bayesian attenuation tomography to the MDAC methodology (Tarantola, 1987; Taylor et al., 2003). Tomographic results from prior studies can be used or built upon using a Bayesian approach that accounts for inadequacies of the assumption of a constant Q_0 for a large region. The advantages of a Bayesian approach to tomography are that large-scale and high-resolution tomographic models available from other well-accepted studies can be used as prior background models. The resulting refined tomographic model blends into these prior background models. Moreover, the error budget is well established in a Bayesian framework. We assume a general linear Gaussian (least squares) model, where the covariance matrix is partitioned into data and prior model components. Uncertain data are naturally down-weighted, and certain model components will be subject to small perturbations.

An advantage of the Bayesian approach to tomography is that the posterior model will blend into the prior background model. The prior model can be a well-accepted global model that can contain constraints from detailed studies in specific regions. For example, Xie (2002) included results from PASSCAL experiments within Tibet that suggest attenuation within the plateau is greater than that calculated using data crossing the entire plateau (which may be due to a data censoring problem discussed below). Additionally, Fan and Lay (2002) suggest that apparent blockage of Lg in Tibet may be due to strong crustal attenuation in northern Tibet, although blockages are known to exist elsewhere (e.g., Baumgardt, 1990; Zhang and Lay, 1995). In the study of Taylor et al. (2003), we used the Eurasia Lg coda Q model and associated errors of Mitchell et al. (1997) as the prior attenuation and covariance model **(**Equation 13).

Figure 1 shows an example of a 1 Hz Lg tomographic Q model for eastern Asia that blends into the *a priori* Eurasian Lg coda Q model of Mitchell et al. (1997). The eastern Asia model was computed using 2^o cells (as opposed to 3^o cells for the Mitchell model) because of the addition of many more amplitude measurements and stations. Subsequent high-resolution models have been developed having 1^o cells.

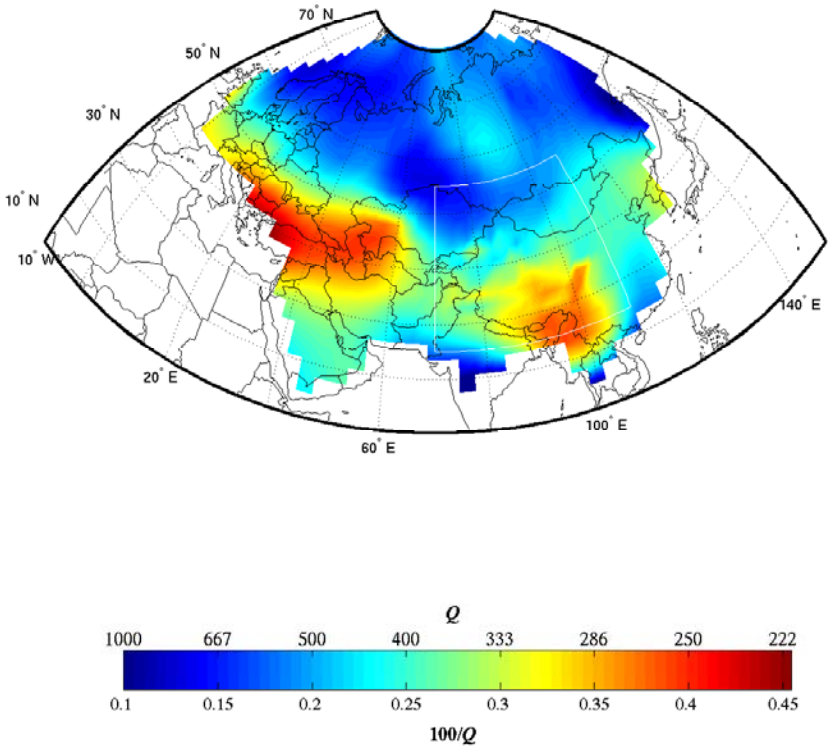

Figure 1. Two degree attenuation tomography map for 1 Hz Lg of Figure 2 (white outline) blending into 3 degree Lg coda Q map of Mitchell et al. (1997).

An alternative approach using the Bayesian framework is to perform a two-stage inversion as suggested by Yang et al., (2004; Figure 2), where the *a priori* model comes from a coarse grid tomographic model using interstation amplitude ratios. The results will then be used as the *a priori* in the single-station amplitude inversion to obtain the final attenuation model. Of course, many effects common to both stations, such as Mw drop out resulting in more stable measurements.

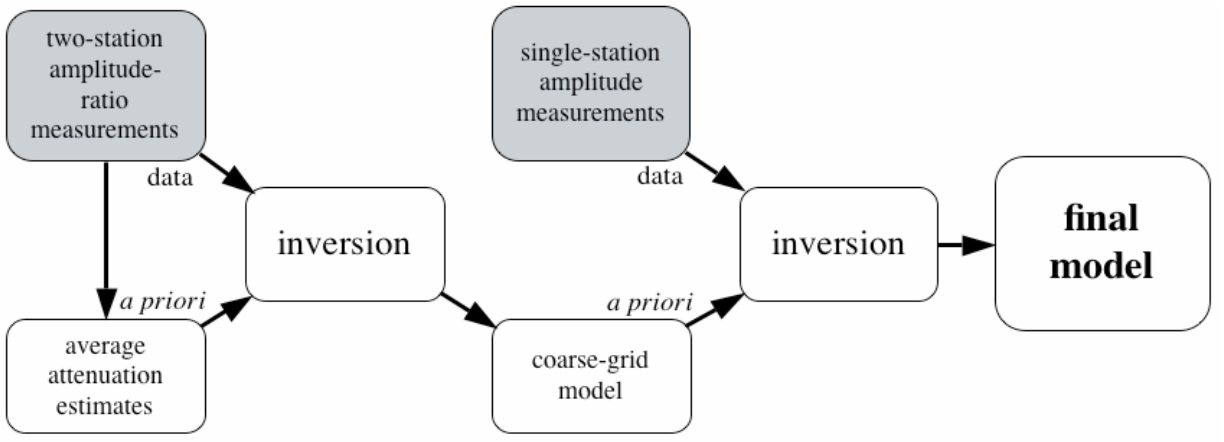

Figure 2. Flowchart of the two-stage tomographic inversion.

Amplitude tomography provides only an approximation to the propagation effects a seismic wave may experience. It is well known that there exist significant tradeoffs between geometric spreading and attenuation. For example, geometric spreading factors for Pn can vary with range and frequency, depending on the velocity structure (e.g., Sereno and Given, 1990). In contrast, Yang (2002) found that Lg geometrical spreading is independent of frequency

for a wide range of velocity models. Thus, the emphasis of this study will be to examine effects of crust and upper mantle structure on the transition zone distances of local to regional (e.g. Pg to Pn) and far-regional to teleseismic (Pn to teleseismic P) at 1 Hz. This far-regional to teleseismic transition is important for making a seamless tie between regional and teleseismic discriminants.

Upper mantle velocity structure plays an important role in determining the complexity of far-regional and near-teleseismic waveforms. In general, a low-velocity zone (LVZ) exists between about 100–200 km depth. Below the LVZ, *P*- and *S*-wave velocities increase smoothly through the upper mantle, to a depth of approximately 410 km. The mantle transition zone, between about 400–700 km depth contains discontinuities near 410 km and 660 km, where the velocities increase rapidly. Plots of the IASP91 (Kennett and Engdahl, 1991) and JB (Jeffreys and Bullen, 1958) velocity structures for the mantle and the transition zone are shown in Figure 3. These discontinuities cause *triplications* in the travel time curve, as shown in Figure 4. Although these regions are often referred to as the 410- and 660-km discontinuities, their exact depths vary from region to region.

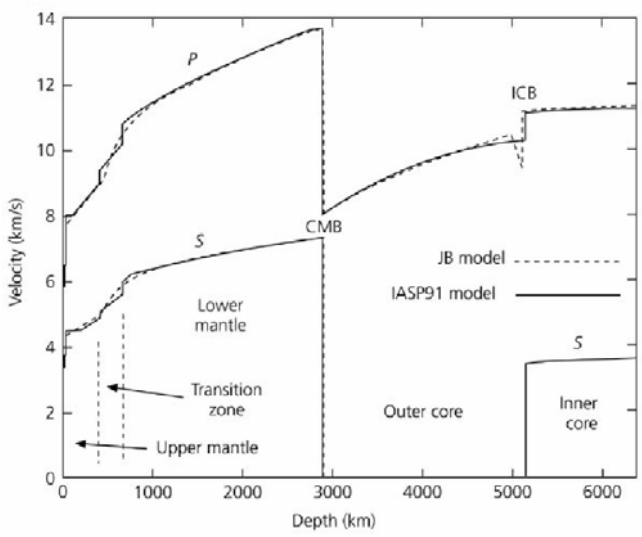

Figure 3. P- and S-wave velocity models for the earth showing the sharp discontinuities in the upper mantle transition zone (from Stein and Wysession, 2002).

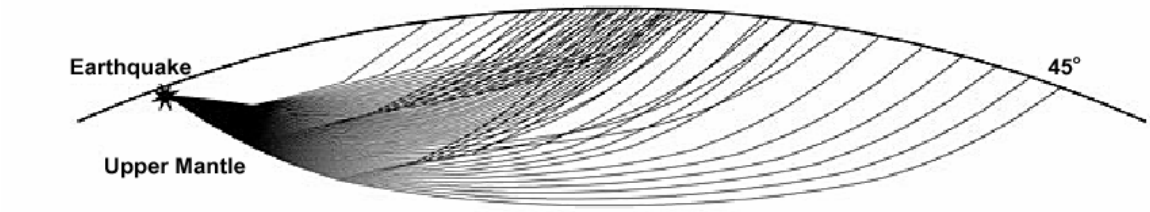

Figure 4. Illustration of the effects of triplication on ray paths between 17° to 23° epicentral distance (from Stein and Wysession, 2002).

Many of the regional monitoring methodologies currently employed, such as kriged amplitude and travel-time correction surfaces, were developed for regions *in between* the *Pn-Pg* and the *Pn-P* crossover distances, leaving two important distance ranges uncalibrated in terms of realistic physical models that explain the observed effects of triplication, phase blockage, and lateral heterogeneity. The latter of these distance ranges is at far-regional/near-teleseismic distances (13° to 30°), where the crossover occurs between *Pn* to *P* as the first arrival on seismograms. At this distance, *P*-waves bottom between the Moho and 660 km. Accurate velocity models are required for the region of interest in order to identify the phase as *Pn*, *P, Pdiff, PP,* their shear-wave equivalents, and possible precursors, and to accurately locate events, which can be very problematic given a small event recorded on a sparse

network. Perhaps the only way to correctly identify each phase is through accurate travel-time prediction and/or improved array processing. In addition, triplication can result in a focusing of the *P*- and *S*-wave energy, resulting in anomalous amplitudes, incorrect magnitude estimates, and inaccurate phase ratio discriminant performance.

As discussed above, the MDAC method was originally developed for distances between the *Pg*-*Pn* crossover (< 5°) and the *Pn*-*P* crossover (> 17°). One of the objectives of this proposal is to use the information gathered in studies of transition-zone amplitude anomalies observed at regional arrays to extend MDAC outside of its currently defined distance range. As a first step, we will investigate the geometrical spreading term in Equation 1 which is defined following Street et al. (1975) with a critical distance R_o within which the spreading is spherical and beyond which it decays as distance to the power η

$$G(R) = \begin{cases} \dfrac{1}{R} & \text{where} \quad R < R_o \\ \dfrac{1}{R_o}\left(\dfrac{R_o}{R}\right)^{\eta} & \text{where} \quad R \geq R_o \end{cases} \qquad (1)$$

This formulation accounts for the crustal waveguide effect on some phases, such as *Pg* and *Lg*. For upper mantle phases *Pn* and *Sn*, we can set R_o to a small number (e.g., 1 km). Because MDAC is a station-centric amplitude correction method, the simple frequency-independent geometric spreading correction is going to be inadequate at transition-zone distances for *P* (and *S*) waves. Additionally, geometric spreading factors for a particular phase can vary with range and frequency depending on the velocity structure (e.g., Sereno and Given, 1990). The geometric spreading can be particularly affected at transition-zone distances where triplications occur. This is illustrated in Figure 5, which shows kriged 1 Hz *Pn* amplitude residuals calculated using a simple geometric spreading model normalized for source amplitude from station LZH. From this figure it can be seen that amplitudes show a distinctive ringed pattern moving outward from LZH. In particular, there is a change in amplitudes from low to high of 0.1 to 0.2 magnitude units out at approximately the 20-degree transition region. This suggests that a simple geometric spreading representation such as that used in Equation 1 can only match amplitude decay to the first order for *Pn*. Using the phase arrival database and the mapped amplitude variations for each station relative to the MDAC model, we will work to extend MDAC to the far-regional distance range. As part of this task, UCSC and LANL will investigate improved geometric spreading representations that capture the phenomenology of the *Pg* to *Pn* and *Pn* to teleseismic *P* transition zones.

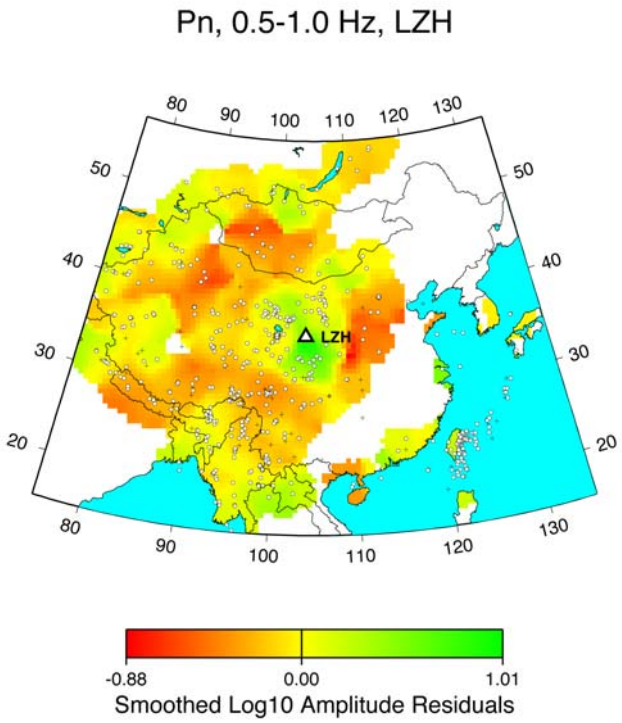

Figure 5. Kriged 1 Hz Pn amplitude residuals normalized for source amplitude from station LZH (Lanzhou, China).

Additionally, phase blockage can occur over relatively short distances in the absence of any anelastic effects (e.g., McNamara et al., 1996; Rapine et al., 1997). Station-centric kriged amplitude correction surfaces on top of the tomographic models may assist in identifying blocked paths (e.g., Phillips, 1999; Rodgers et al., 1999) as well as deficiencies in geometrical spreading representations.

Waveform Data Collection

We are currently requesting and assembling waveform data from the Incorporated Research Institute for Seismology (IRIS) Data Management Center (DMC) and LANL Database to prepare for phase picking and amplitude measurement. We have selected about 100 broadband and short-period stations in the region for the data collection. Figure 6 shows the distribution of the stations. We have removed some stations from the initial selection because of their proximity to each other (< 2º).

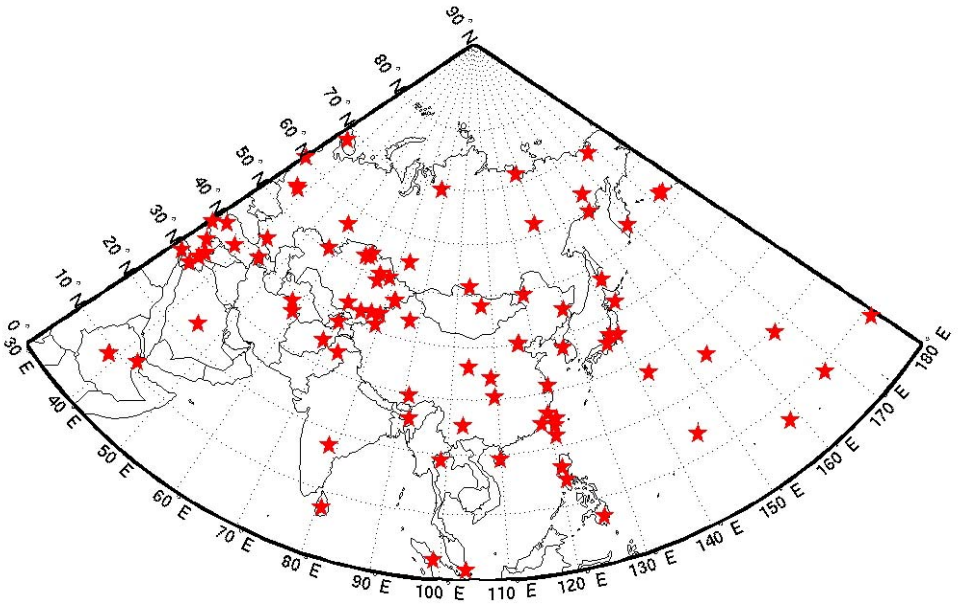

Figure 6. Station distribution for the data collection.

Figure 7 plots the seismic events that we initially selected for our data requests. These are events that occurred between 1975 and 2004, have magnitudes of 3 or larger and have depths of 50 km or shallower. From the histogram in the figure, we can see severe event clustering along the West Pacific Rim. These event clusters would potentially bias the path coverage for our later inversion. To decluster the events, we divided the whole region into 1-by-1º cells and required that the number of events in each cell be no more than one. Events in each cell were ranked based on their magnitudes and the number of stations that might have recorded the events (estimated from source-receiver distances and operation status of the stations). Although the area of the cells is different for different latitudes, the difference becomes significant only when we approach the North Pole, where the events are so scattered that we did not want to remove too many events in this region anyway. Additional criteria, such as a source-receiver distance of 4000 km or shorter, etc., are imposed in formulating the data requests. A total of 3796 events were selected. Figure 7 shows the distribution of final event selection that was used in the data request. Depending on the actual number and quality of waveforms that we obtain, we will reevaluate our criteria and make adjustments to relax some of the criteria if necessary.

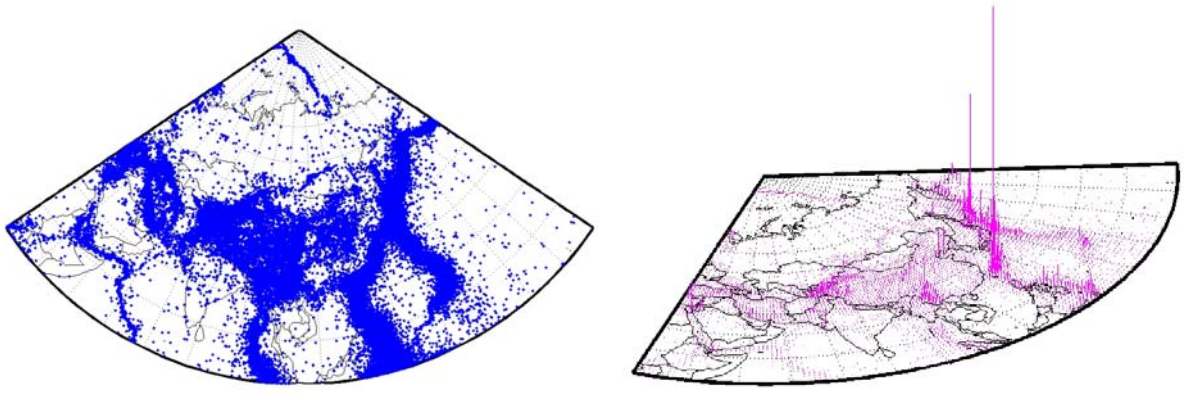

Figure 7. Events that passed initial selection criteria of magnitude and depth. The plot on the right is a three-dimensional histogram of the number of events in each 1-by-1º cell.

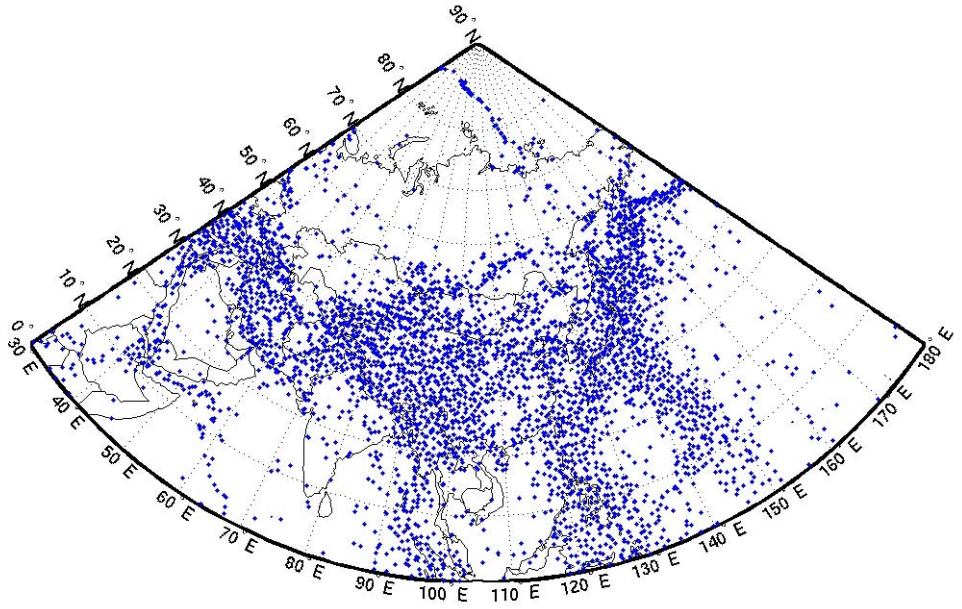

Figure 8. Final event selection used in the data collection. The distribution is much more uniform compared to Figure 7.

CONCLUSIONS AND RECOMMENDATIONS

Underlying geophysical calibration is important for development and improvement of regional seismic discriminants. MDAC amplitude corrections used to develop regional discriminants are critically dependent on such parameters as attenuation and geometrical spreading. This work will address methods to address these issues through a blend of empirical and theoretical techniques.

REFERENCES

Baumgardt, D.R., Investigation of teleseismic Lg blockage and scattering using regional arrays, *Bull. Seism. Soc. Am.*, 80, 2261–2281, 1990.

Fan, G. and T. Lay (2002), Characteristics of Lg attenuation in the Tibetan Plateau, *J. Geophys. Res.* 107: (B10), 2256, doi:10.1029/2001JB000804.

Jeffreys, H. and K. E. Bullen (1958), *Seismological Tables*, British Association for the Advancement of Science, Gray Milne Trust, Office of the British Association, Burlington House, London, England.

Kennett, B. L. N., and E. R. Engdahl (1991), Travel times for global earthquake location and phase identification, *Geophys. J. Int.* 105, 429–465.

McNamara, D.E., T.J Owens, and W.R. Walter, Propagation characteristics of Lg across the Tibetan Plateau, *Bull. Seism. Soc. Am.* 86: 457–469, 1996.

Mitchell, B.J., Y.Pan, J. Xie (1997), and L. Cong, Lg coda Q variation across Eurasia and its relation to crustal evolution, *J. Geophys. Res.* 102: (22),767–22,779.

Phillips, W. S. (1999), Empirical path corrections for regional-phase amplitudes, *Bull. Seism. Soc. Am.* 89: 384-393.

Rapine, R. R. J. F. Ni, and T. M Hearn (1997), Regional wave propagation in China and its surrounding regions, *Bull. Seism. Soc. Am.* 87: 1622–1636.

Rodgers, A. J., W. R. Walter, C. A. Schultz, S. C. Myers, and T. Lay (1999), A comparison of methodologies for representing path effects on regional P/S discriminants, *Bull. Seism. Soc. Am.* 89: 394–408.

Sereno, T. J. and J. W. Given (1990), Pn attenuation for a spherically symmetric earth model, *Geophys. Res. Lett.* 17, 1141–1144.

Stein, S. and M. Wysession (2002), *An Introduction to Seismology, Earthquakes and Earth Structure*, Blackwell Science, Inc.

Street, R., R. Herrmann, and O. Nuttli (1975), Spectral characteristics of the Lg wave generated by central United States earthquakes, *Geophys. J. R. Astron. Soc.* 41: 51–63.

Tarantola, A. (1987), *Inverse Problem Theory*, Elsevier Science, Amsterdam, The Netherlands.

Taylor, S. R., and H. E. Hartse (1998), A procedure for estimation of source and propagation amplitude corrections for regional seismic discriminants, *J. Geophys. Res.* 103: 2781–2789.

Taylor, S. R., A. A. Velasco, H. E. Hartse, W. S. Phillips (2002), W.R. Walter, and A.J. Rodgers, Amplitude corrections for regional seismic discriminants, *Pure. App. Geophys. 159*: 623–650.

Taylor, S. R., X. Yang and W. S. Phillips (2003). Bayesian Lg attenuation tomography applied to eastern Asia, *Bull. Seism. Soc. Am.* 93: 795–803.

Walter, W. R. and S. R. Taylor (2002), A revised Magnitude and Distance Amplitude Correction (MDAC2) procedure for regional seismic discriminants: Theory and testing at NTS, Los Alamos National Laboratory document LA-UR-02-1008.

Yang, X., A numerical investigation of Lg geometrical spreading, *Bull. Seism. Soc. Am.* 92, 3067–3079, 2002.

Yang, X., S.R. Taylor, and H.J. Patton (2004), 20-sec Rayleigh-wave attenuation tomography for central and southeast Asia, *J. Geophys. Res*. 109 B12.

Xie, J. (2002), Lg Q in the eastern Tibetan Plateau, *Bull. Seism. Soc. Am.* 92: 871–876.

Zhang, T., and T. Lay (1995), Why the Lg phase does not traverse oceanic crust, *Bull. Seism. Soc. Am.* 85 1665–1678.